Superconducting Magnets for Ultra Light and Magnetically Shielded, Compact Cyclotrons for Medical, Scientific, and Security Applications

Alexey Radovinsky, Joseph V. Minervini, *Member, IEEE*, Craig E. Miller, Leslie Bromberg, Philip C. Michael, and Mario Maggiore

***Abstract*—We show that multiple sets of superconducting coils can be used to generate the magnetic field profile required in a synchrocyclotron, replacing the ferromagnetic pole pieces typically used in these machines. Coil number, location, and current are adjusted to produce the required field for particle acceleration. Superconducting coils are likewise used to magnetically shield the device, eliminating the need for a ferromagnetic return yoke or ferromagnetic shields. The results demonstrate several significant advantages for a design that eliminates the iron yoke and poles and relies instead on high performance superconducting coils for local field shaping and for magnetic shielding.**

***Index Terms*—Cyclotrons, magnetic shielding, particle accelerators, superconducting coils.**

I. Introduction

SUPERCONDUCTING cyclotrons are used for cancer treatment, nuclear medicine, ion implantation, nuclear materials testing, and national security [1]–[6]. The use of superconductivity in a cyclotron design can reduce its mass by about an order of magnitude, yielding a significant reduction in overall cost [2], [7], [8]. Despite nearly 40 years of design effort [7]–[10] the basic magnetic configuration for superconducting cyclotrons remains relatively unchanged from that proposed by Lawrence over 80 years ago for resistive-magnet-based cyclotrons [11]. The basic configuration still consists of a single, split pair solenoid embedded in a relatively massive iron return yoke, with the radial magnetic field profile in the acceleration region produced by a pair of magnetically saturated iron poles. The use of a warm iron yoke also requires the transmission of substantial electromagnetic loads across the cryostat boundary; these loads must be accommodated in the cryogenic design of the magnet vessel.

Manuscript received July 28, 2013; accepted October 17, 2013. Date of publication November 5, 2013; date of current version February 14, 2014. This work was supported in part by the Los Alamos National Laboratory under Subcontract Number 212197.

J. V. Minervini is with the Plasma Science and Fusion Center, MIT, Cambridge, MA 02139 USA (e-mail: minervini@psfc.mit.edu).

A. Radovinsky, L. Bromberg, C. E. Miller, and P. C. Michael are with the Plasma Science and Fusion Center, MIT, Cambridge, MA 02139 USA (e-mail: radovinsky@psfc.mit.edu; brom@psfc.mit.edu; cemiller@psfc.mit.edu; michael@psfc.mit.edu).

M. Maggiore is with the Laboratori Nazionali di Legnaro, National Institute of Nuclear Physics (INFN), 35020 Padova, Italy (e-mail: mario.maggiore@lnl.infn.it).

Color versions of one or more of the figures in this paper are available online at http://ieeexplore.ieee.org.

Digital Object Identifier 10.1109/TASC.2013.2287853

Previous design studies to address design limitations imposed by reliance on iron based technology concentrated primarily on isochronous machines. These studies examined the replacement of the iron poles with shaped superconducting coils as a means to enhance the flutter field achievable in a high field device [12], [13].

In this paper, we present a conceptual design for a compact superconducting synchrocyclotron that demonstrates the possibility to reduce its weight significantly by eliminating all iron from the design. Ultra-light-weight, highly portable particle accelerators are desirable for some national security applications as well as for gantry mounted radiotherapy machines [4], [6]. Proposed implementation of this design benefits from several significant advances in superconducting magnet technology pioneered in the magnetic resonance imaging (MRI) industry during the past 20 years, such as active magnetic shielding [14]. In addition to the prospect of reduced weight, improved portability, enhanced magnetic shielding and structural efficiency, the proposed approach introduces the possibility to continuously vary the output beam energy without need for an external energy degrader.

II. Conceptual Design of the Magnet System for an Iron-Free Superconducting Synchrocylotron

In this section of the paper we briefly describe the magnetic design for an iron-based, 9 T, 250 MeV synchrocyclotron that our group developed a few years ago, which was commercialized as the Mevion Medical Systems Inc. (formerly Still River Systems Inc.) Monarch 250 [3], [15]. We will refer to this as our reference design. We then proceed to present the magnetic design for an iron-free equivalent [16], before comparing key design parameters for both designs.

A. Reference Design

Fig. 1 shows a simplified, 1/4 section view of our reference design [17]. The superconducting coil pair is wound using a four-strand, pre-reacted Nb_3Sn cable in channel conductor and generates a magnetic flux density of 9 T near the center of the cyclotron. The coils are housed in a stainless steel bobbin that reacts the electromagnetic loads and helps to position the coils with respect to the iron yoke and pole tips. The coils are protected during quench by a combination of an external dump resistor and quench propagation heaters embedded in the windings. The heaters are triggered by cold diodes during

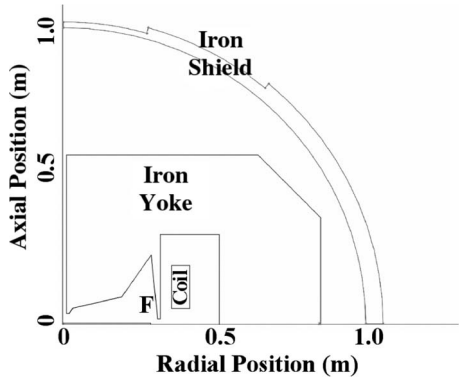

Fig. 1. View (1/4-section) of the 250 MeV reference design. The design includes a "finger," (F), to alter the field profile near the edge of the pole to facilitate beam extraction, and an iron shield to further reduce the fringe magnetic field near the device.

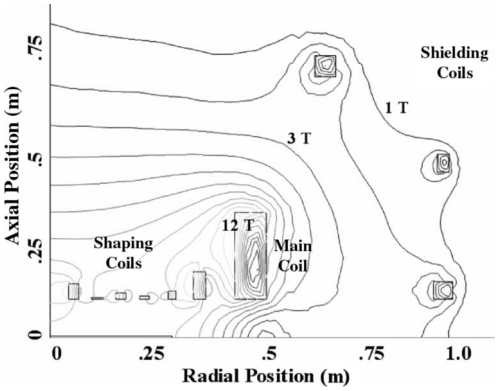

Fig. 2. Contours of magnetic field for the 250 MeV iron-free design, using a main field coil, six field shaping coils and three shielding coils.

the start of the quench dump. The engineering current density, including insulation, is roughly 200 A-mm^{-2}, while the peak quench temperature is roughly 200 K.

B. Equivalent Iron-Free Synchrocyclotron Design

Fig. 2 shows a 1/4 section view of the magnetic field configuration for an equivalent magnetic design for the synchrocylotron, where the iron yoke and poles are replaced by superconducting coils. The iron-free design was produced using an iterative solver. The design is for illustrative purposes, to examine the basic feasibility of the proposed approach. Additional iterations would be needed to optimize the design for a working device.

For this example, the solver used a single pair of main field coils and six pairs of field shaping coils to match the radial magnetic flux density across the midplane of the acceleration region with that for the reference design. The design also used three pairs of magnetic shielding coils to satisfy preselected fringe field values in the far field. The plot in Fig. 3 shows that the magnetic field profile across the midplane of the cyclotron for the iron-free design is nearly identical to that for the reference design.

The coil positions, radial widths and the magnitude but not direction of the current density were fixed for each iteration; the program then adjusted the axial heights of the coils to minimize the deviation from the target field. The use of constant,

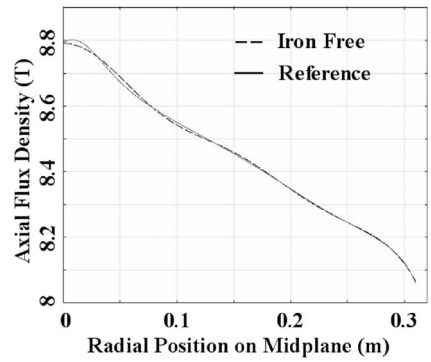

Fig. 3. Axial magnetic flux density versus radial position at the cyclotron midplane for the reference design (Fig. 1), overlaid with that for the equivalent iron-free cyclotron, shown in Fig. 2.

TABLE I
RON-FREE 250 MeV COIL CONFIGURATION

Coil #	Rc (m)	Zc (m)	ΔR (m)	ΔZ (m)	J (A/mm^2)
1	0.510	0.212	0.080	0.223	235.9
2	0.060	0.120	0.026	0.039	235.9
3	0.120	0.102	0.030	0.004	-235.9
4	0.180	0.108	0.026	0.016	235.9
5	0.240	0.104	0.024	0.008	235.9
6	0.310	0.110	0.020	0.021	-235.9
7	0.380	0.135	0.031	0.070	235.9
8	0.700	0.700	0.053	0.054	-235.9
9	1.000	0.450	0.031	0.046	-235.9
10	1.000	0.122	0.049	0.045	-235.9

Coil identification: 1 – Main coil, 2-7 – Shaping coils, 8-10 – Shielding coils

235 A-mm^{-2} current density presupposes that the coils are connected in series and that the same superconducting cable is used for all coils. The axial and radial positions of the coil centers are summarized in Table I, along with their axial and radial builds. The separation between magnetic flux density contours in Fig. 2 is 1 T. The main coil has a peak magnetic flux density of about 12 T, roughly 1 T higher than in the reference design. The field shaping coils have magnetic flux densities slightly smaller than that for the main coil. The shielding coils, on the other hand, have magnetic flux densities lower than about 5 T.

We developed a rudimentary support structure to complete the design. The stainless steel structure was sized to support the computed electromagnetic loads and to facilitate determination of the magnet system weight. To permit further optimization of the coil support structure and cryostat, the vertical distance from the cyclotron midplane to the near edge of the superconducting coils for the iron-free design was increased to 10 cm from the 7 cm distance used in the reference design.

The quench protection circuit would be similar to that used for the referenced design, with suitable modification to account for the inductive coupling present in a multi-coil system [14]. A normal zone anywhere in the magnet system would be actively detected and used both to trigger current dump through an external resistor and to activate quench propagation heaters embedded in each coil in the magnet system.

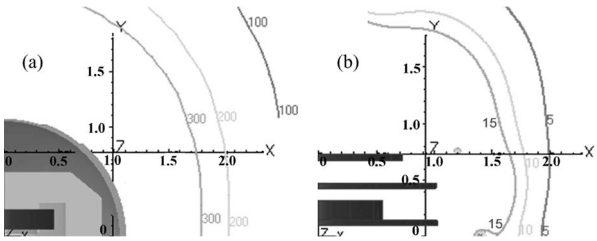

Fig. 4. Fringe magnetic field contours for: (a) the reference synchrocyclotron design and (b) the iron-free design.

TABLE II
KEY PARAMETERS FOR THE REFERENCE AND IRON-FREE SYNCYROCYCLOTRON DESIGNS

Parameter	250 MeV reference design	Iron-free equivalent
Ion species	H^+	H^+
Beam energy [MeV]	253	253
Beam extraction radius [m]	0.3	0.3
Central magnetic flux density [T]	8.8	8.8
Peak magnetic flux density on superconductor winding [T]	10.7	12.4
Overall current density [A mm^{-2}]	200	235
Stored magnetic energy [MJ]	9.7	30.3
Magnet system weight [kg]	24,500	4,000
Fringe field @ 2 m midplane radius [G]	209	4
Fringe field @ 2 m on-axis distance [G]	416	13

C. Design Comparison and Future Optimization

Although the axial and radial distances to the shielding coils were constrained by the program to remain within the boundaries of the iron yoke from the reference design, Fig. 4 shows that the fringe field without iron decreases much faster with distance than that for the reference design. The 5 gauss contour for the iron-free design [Fig. 4(b)] occurs about 2 m from the coil center, while that for the reference design is about 6 m away from the coil center.

Table II summarizes key parameters for the reference synchrocyclotron design and its iron-free equivalent. The results in Table II indicate that, for the example shown, it was possible to decrease the weight of the cyclotron magnet system by a factor of about six, from roughly 24.5 tons to about 4 tons, by eliminating all iron from the design. The weight listed for the iron-free design in Table II includes that for the coils, the coil support structure, and the larger sized cryostat needed to enclose the shielding coils.

Conversely, the marked reduction in system weight in Table II comes at the cost of significant increase in the peak magnetic flux density in the winding, from 10.7 T to nearly 12.4 T, and in the stored magnetic energy, from roughly 9.7 MJ to roughly 30.3 MJ. The extent of these increases is due to the specifics of the design example. For instance, the peak field in the windings can be reduced in subsequent design iterations by relaxing the constraints on the fringe field and allowing the 5 gauss line to move further out from the magnet center. The stored magnetic energy could be similarly reduced both by relaxing the constraints on the fringe field and by reducing the vertical distance to the main and field shaping coils to a value closer to that used in the reference design.

III. PERCEIVED ADVANTAGES TO THE IRON-FREE DESIGN

A. Reduced Weight and Enhanced Portability

The conceptual iron-free design demonstrates that it is technically feasible to substantially decrease the weight of a synchrocyclotron by eliminating all iron from the design. The weight of the coils, support structure, and cryostat that are needed to replace the iron is only a small fraction of the weight of the iron that they replace.

To facilitate the direct replacement of our reference cyclotron with an iron-free equivalent, we chose to limit the placement of the outermost layer of shielding coils to roughly the same locations as the edges of the iron yoke that they replaced, so that the system volume would not increase. This consideration greatly simplifies the development of iron-free cyclotrons for systems that require transportability, gross movement, or rotation of the cyclotron about a patient treatment isocenter [2], [4]. Reducing the weight of a gantry mounted cyclotron permits a significant, corresponding reduction in the weight of the gantry as well.

B. Variable Energy Acceleration in a Single Device

A second, very attractive feature facilitated by the development of iron-free synchrocyclotrons is the possibility to vary the output energy from the device without resorting to an energy degrader. Reliance on energy degraders comes at the cost of undesirable production of secondary radiation that markedly increases the radiation shielding required for placement in a patient treatment environment [18].

Changing the energy of the synchrocyclotron beam, while maintaining the same extraction radius, requires a change in the magnetic flux density of the device, but not its normalized field profile. Because there is no saturable iron, the field profile in the iron-free synchrocyclotron can be scaled up or down linearly, by changing the currents in all coils by the same factor. When all coils are connected in series, this variation is accomplished simply by varying the system current.

Scaling the magnetic flux density in the acceleration region permits ion acceleration from the minimum energy permitted by other subsystems of the cyclotron (ion source, RF system, beam extraction system) to the maximum permitted by the coil design. In an iron-free cyclotron, the beam energy can be adjusted continuously by varying the coil system current, $I_{op}(t)$, as a function of time. By suitable scaling of the frequency and voltage of the acceleration system, the extracted beam can be made to follow the same trajectory regardless of final beam energy, easing requirements on the device's beam targeting system. Other physics issues that must be addressed to accomplish energy variability in conjunction with the magnetic field change are the ion injection and the beam extraction [16].

By comparison, beam energy variation in iron-free isochronous cyclotrons is much more challenging. The magnetic field profile in an isochronous device must simultaneously satisfy two requirements [19]. The azimuthal magnetic flux density variation defining the beam focusing scales linearly with the coil current density. Conversely, the average value of the magnetic flux density at each radial location defining the isochronisms of the beam is functionally related to ion species and final

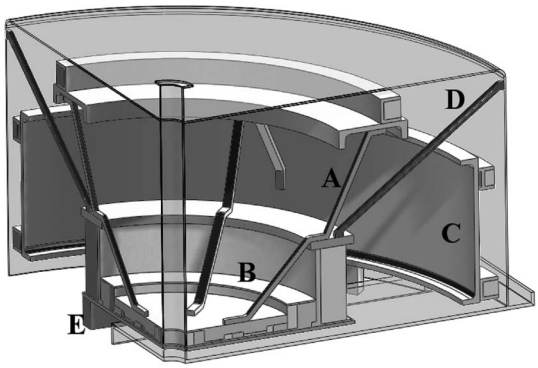

Fig. 5. Triple section view of the coil support system and magnet cryostat.

beam energy. This relation does not scale linearly with the coil current density. Multiple sets of trim coils [10], [20], or trim rods [10], are typically needed to simultaneously fulfill both conditions as beam energy or ion species is varied. Some ideas regarding beam energy variation in an iron-free isochronous cyclotron were previously discussed in [12].

C. Variable Species Acceleration in a Single Device

In addition to changing the beam energy, it is possible to adjust the field and RF frequency and amplitude to accommodate the acceleration of different ion species in a single device. It is thus possible to accelerate hydrogen, deuterium, or carbon in the same cyclotron, but not all of these simultaneously. Such a device would be highly desirable for use in ion beam radiotherapy.

D. Structural Optimization

Fig. 5 shows a conceptual design of the magnet system support and cryostat for the iron-free synchrocylotron presented in Fig. 2. There is no need to transmit electromagnetic loads through the cold-to-warm supports, as in the case of our reference design. The complete containment of electromagnetic loads within the cold mass helps to reduce cryogenic loads, because the cold-to-warm supports need only support the gravity loads on the magnet assembly. The elimination of room temperature iron likewise removes the restriction that the mechanical stiffness of the cold-to-warm supports must exceed the effective magnetic stiffness between coils and iron.

To minimize the weight of the cold mass, the cold mass in Fig. 5 uses a space frame design with pre-tensioned links (A) that are sized to offset lateral and tilt magnetic instabilities between the main and the shaping coils subassembly (B) and the shielding coils subassembly (C). The tension links (D), made of low thermal conductivity material, support the weight of the cold mass from the outer walls of the cryostat. The upper and the lower halves of the cold mass are connected by sturdy compression members (E) that pass through the device's midplane. The cold to warm tension links are pre-tensioned and positioned so that they are always in tension.

E. Field Shaping

Because all electromagnetic loads between the coil pairs are reacted within the cold mass it is possible to precisely align the magnet system at room temperature. Field mapping and coil alignment can be performed at room temperature by applying a modest current to the pre-assembled coil set; this procedure should eliminate manufacturing tolerance related field errors. Once the required field quality is achieved the cold mass would then be set into its cryostat. The alignment procedure needs to account for subsequent dimensional changes due to thermal contraction and deformations from electromagnetic forces and their effect on the field profile. The methods and codes needed to analyze these variations are presently available and are improving all the time.

Using manufacturing methods similar to those developed by MRI magnet vendors [14], it should be possible to achieve less than the approximately 100 ppm harmonic error needed for high efficiency beam extraction [21]. By comparison the magnet system for a whole body MRI typically achieves 10 ppm field homogeneity over a volume extending to half the diameter of the inner most coil [14]. As a consequence, we believe that iron-free designs can be manufactured without the need for magnetic shimming, resulting in a significant decrease in manufacturing effort. If it ultimately turns out that the required field quality cannot be directly built into the iron-free device it will still be possible to adjust the magnetic field profile as needed, using trim coils either inside the cryostat, or at room temperature near the cyclotron midplane.

An iron-free cyclotron will contain several shielding and shaping coil pairs. There are two main options for powering these coils. They can be driven in series, with a single set of current leads. Because the cryogenic heat load is typically dominated by the current lead loads, this operating mode provides the lowest cryogenic heat load. The use of multiple sets of leads increases the flexibility of operation allowing independent adjustment of the currents in different coils to optimize the performance of the machine, at the expense of increased cryogenic heat load. This second option would only be considered in the case of an isochronous machine [12].

F. Conductor Optimization

Some of the coils in our iron-free design, and in particular the shielding coils, could be made from a different type of superconductor than that for the main and field shaping coils. For the case shown in Fig. 2, the peak magnetic flux density in the shielding coils is less than 5 T. At this level of field, more economical NbTi or even MgB_2 operating at a slightly higher temperature could be used for the magnetic shielding coils.

The shielding coils may be part of the cold mass, if they are made using low temperature superconductor, or they can be combined and integrated into the radiation shield if they are made from high temperature superconductors (HTS). Depending on the specific application, it may also be possible to use water-cooled copper shielding coils operating outside the cryostat.

By comparison, the shaping coils, including the main cyclotron coil, have fields on the order of 9 T to 12 T. Thus, the shaping and main cyclotron coils would need to be made from higher performance superconductors, such as Nb_3Sn, or from HTS, such as YBCO.

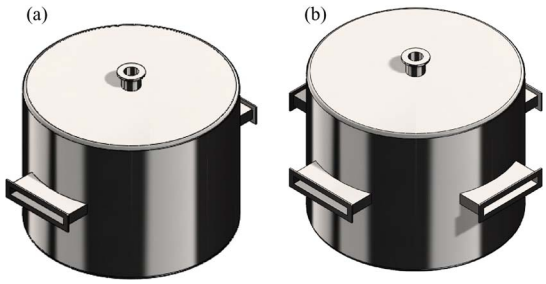

Fig. 6. Perspective views of magnet cryostats with warm cavities for the beam-acceleration subsystems. The cavities facilitate rapid adjustment or maintenance of the beam chamber, using replaceable cassettes. Panel (a) shows a cryostat with a single cavity, while panel (b) shows a cryostat with two orthogonal cavities for greater accessibility.

G. Modular System Design

The elimination of iron from the design allowed us to substantially increase vertical access for the beam chamber at the midplane of the cyclotron. The cryostat shown in Fig. 5 provides a warm vertical access of 10 cm at the cyclotron midplane. Access immediately above and below the central midplane of the cyclotron is likewise improved by the elimination of the iron poles. Improved access to the center of the device should ease maintenance operations on the beam chamber components.

A perspective view of the proposed, iron-free magnet system cryostat is shown in Fig. 6. Room temperature access to the cyclotron midplane is completely isolated from the magnet system by a rectangular slot (or slots) which pass horizontally through the cryostat at the height of the magnet system midplane, as part of the cryostat vacuum boundary. The slots facilitate a modular design approach whereby the beam acceleration subsystems, including the ion source, radio frequency acceleration structures, and beam extraction system, are incorporated into a separate, vacuum-tight cassette that is inserted into and referenced to the slots. By use of this modular approach it should be possible to easily exchange one cassette for another, for example to change between ion sources or species, to modify internal targets, alter the beam accelerating structures, and to service or repair any other subsystem component as required.

IV. Conclusion

The use of iron in early cyclotron designs was an obvious choice because of the significant reduction it allowed in the required numbers of ampere-turns of resistive conductor. The rational to retain iron in present high field designs is not as obvious.

We have recently investigated the possibility to completely eliminate iron from the design of a superconducting synchrocyclotron as a means to dramatically improve performance. Reduced weight and more effective shielding, could lead to the deployment of ultra-light weight cyclotrons on mobile platforms. Iron-free designs should also be easier to tune in mass production. Increased access to the central midplane of the device should permit modular design of the beam acceleration chamber, for example, by use of removable cassettes.

The iron-free cyclotron design approach proposed here uses multiple sets of superconducting coils to generate the magnetic field profile needed for particle acceleration as well as to actively shield the environment from the device's fringe magnetic field. This design approach can be viewed as an extension to cyclotron design of the field analysis and magnet construction techniques pioneered in the MRI industry during the past few decades. Although we focused on synchrocyclotrons in this paper, many of the issues discussed here are equally applicable to the design of isochronous machines.

References

[1] M. K. Craddock and K. R. Symon, "Cyclotrons and fixed-field alternating-gradient accelerators," *Rev. Accel. Sci. Technol.*, vol. 1, no. 1, pp. 65–97, Jan. 2008.

[2] S. Peggs, T. Satogawa, and J. Flanz, "A survey of hadron therapy accelerator technologies," in *Proc. IEEE Part. Accel. Conf.*, 2007, pp. 115–119.

[3] J. N. A. Matthews, "Accelerators shrink to meet growing demand for proton therapy," *Phys. Today*, vol. 62, no. 3, pp. 22–24, Mar. 2009.

[4] A. R. Smith, "Vision 20/20: Proton therapy," *Med. Phys.*, vol. 6, no. 2, pp. 556–568, Feb. 2009.

[5] G. M. Wright, H. S. Barnard, Z. S. Hartwig, P. W. Stahle, R. M. Sullivan, K. B. Woller, and D. G. Whyte, "Plasma-surface interaction research at the Cambridge laboratory of accelerator studies of surfaces," in *Proc. 21st AIP Conf. Appl. Accel. Res. Ind.*, 2011, pp. 626–630.

[6] R. C. Lanza and T. A. Antaya, "High energy protons for remote standoff detection of special nuclear materials," in *Proc. 11th Int. Conf. Appl. Nucl. Tech.*, 2011, pp. 153–160.

[7] H. R. Schneider, J. S. Fraser, and C. B. Bigham, "Superconducting cyclotrons," *IEEE Trans. Magn.*, vol. MAG-11, no. 2, pp. 443–446, Mar. 1975.

[8] D. Krischel, C. Buamgarten, A. Geisler, A. Hobl, H.-U. Klein, M. Poier, H. ROcken, M. Schillo, P. Vom Stein, T. Stephani, J. H. Timmer, and C. Zimmer, "Design aspects and operation experience with a novel superconducting cyclotron for cancer treatment," *IEEE Trans. Appl. Supercond.*, vol. 17, no. 2, pp. 2307–2310, Jun. 2007.

[9] C. R. Hoffman, C. B. Bigham, J. S. Fraser, E. A. Heighway, J. A. Hulbert, J. H. Ormrod, and H. R. Schneider, "The chalk river heavy ion superconducting cyclotron," *IEEE Trans. Nucl. Sci.*, vol. NS-22, no. 3, pp. 1647–1650, Jun. 1975.

[10] H. G. Blosser, "The Michigan State University superconducting cyclotron program," *IEEE Trans. Nucl. Sci.*, vol. NS-26, no. 2, pp. 2040–2047, Apr. 1979.

[11] E. O. Lawrence and M. S. Livingstone, "The production of high speed light ions without the use of high voltages," *Phys. Rev.*, vol. 40, no. 19, pp. 19–35, Apr. 1932.

[12] K. M. Subotic, "Multipurpose air-core superconducting cyclotrons," in *Proc. IEEE SC X Int. Conf. Cyclotrons Appl.*, East Lansing, MI, USA, 1984, pp. 469–471.

[13] H. Ueda, M. Fukuda, K. Hatanaka, T. Wang, X. Wang, A. Ishiyama, S. Noguchi, S. Nagaya, N. Kashima, and N. Miyahara, "Conceptual design of next generation HTS cyclotron," *IEEE Trans. Appl. Supercond.*, vol. 23, no. 13, p. 4100205, Jun. 2013.

[14] Y. Lvovsky, E. W. Stautner, and T. Zhang, "Novel technologies and configurations of superconducting magnets for MRI," *Supercond. Sci. Technol.*, vol. 26, no. 9, pp. 1–71, Sep. 2013.

[15] A. Radovinsky, "Baseline magnetic design, k250z3n-4mu-b1," in *K250 Project Memo*. Cambridge, MA, USA: MIT-Plasma Science and Fusion Center, Nov. 27, 2007.

[16] A. L. Radovinsky, J. V. Minervini, P. C. Michael, L. Bromberg, and C. E. Miller, "Variable energy acceleration in a single iron-free synchrocyclotron," MIT Plasma Sci. Fusion Center Res. Rep., Cambridge, MA, USA, PSFC/RR-13-9, Sep. 2013.

[17] T. A. Antaya, A. L. Radovinsky, J. H. Schultz, P. H. Titus, B. A. Smith, and L. Bromberg, "Magnet structure for particle acceleration," U.S. Patent 7 656 258, Feb. 2, 2010.

[18] F. Stichelbaut, T. Canon, and Y. Jongen, "Shielding studies for a hadron therapy center," *Nucl. Technol.*, vol. 168, no. 2, pp. 477–481, Nov. 2009.

[19] H. G. Blosser and D. A. Johnson, "Focusing properties of superconduting cyclotron magnets," *Nucl. Instrum. Methods*, vol. 121, no. 2, pp. 301–306, Oct. 1994.

[20] D. L. Friesel, W. P. Jones, and E. A. Kowalski, "Isochronism studies at IUCF," *IEEE Trans. Nucl. Sci.*, vol. NS-26, no. 2, pp. 2408–2410, Apr. 1979.

[21] J. Van de Walle, W. Kleeven, C. L'Abbate, V. Nuttens, Y. Paradis, M. Conjat, J. Mandrillon, and P. Mandrillon, "Mapping of the new IBA superconducting synchrocyclotron (S2C2) for proton therapy," presented at the Cyclotrons, Vancouver, BC, Canada, Sep. 2013, Paper TU4PB01.